

Bearing and deformation characteristics of geotextile-encased granular piles using recycled solid waste

L. Sun¹, R. Lang², S. Feng³, H. Zhao⁴ and Y. Tian⁵

¹Tianjin University, 92 Weijin Road, Nankai District, Tianjin, China; email: sunlg@tju.edu.cn

²Key Laboratory of Soft Soil Engineering Character and Engineering Environment of Tianjin, Tianjin Chengjian University, 26 Jinjing Road, Xiqing District, Tianjin, China; email: tcuqrq@163.com

³Anhui Zhongyi New Material Science and Technology Co.,LTD., Chuzhou, Anhui, China; email: fsz@163.vip.com

⁴Tianjin University, 92 Weijin Road, Nankai District, Tianjin, China; email: zhaohuan17@tju.edu.cn

⁵The University of Melbourne, Grattan St, Parkville, Victoria 3010; email: yinghui.tian@unimelb.edu.au

ABSTRACT

This study introduces a novel geotextile-encased granular pile made from recycled solid waste. Through uniaxial compression tests, the effects of soil relative density, particle size, and geotextile tensile strength on pile strength and modulus were examined. Among these, geotextile tensile strength had the most significant impact. Particles larger than 3cm were found to reduce pile strength due to puncturing and crushing. Model tests in soft clay revealed that geotextile-encased solid waste granular piles outperformed traditional piles, achieving a 72% reduction in settlement and a 176% increase in pile-soil stress ratio. This enhanced design not only improves mechanical properties but also promotes economic savings and emission reductions, offering a promising solution for sustainable construction practices.

Keywords: granular pile, geotextile, solid waste material, bearing capacity, model test

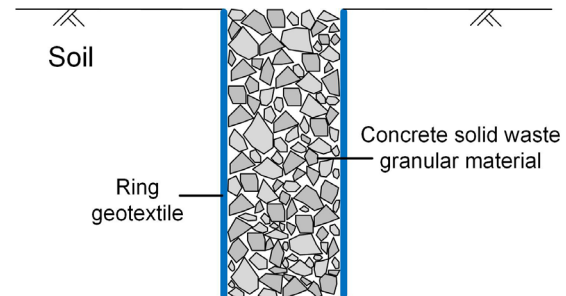
1 INTRODUCTION

The rapid expansion of urban construction has led to a significant increase in construction solid waste, contributing to resource wastage and environmental pollution. This waste predominantly consists of concrete, bricks, wood, metal, and glass, with concrete comprising over 60%. Repurposing construction solid waste offers substantial benefits, including reducing carbon emissions, economic savings, and environmental protection, thus holding great potential for sustainable development.

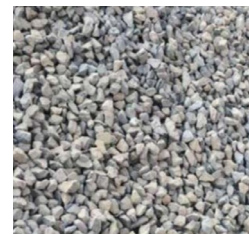
An innovative method to utilize construction solid waste is through the creation of granular piles. While traditional granular piles are effective for ground improvement, they often experience bulging failure under axial loads (Raithel et al., 2004). In contrast, geotextile-encased granular piles provide enhanced performance by limiting lateral deformation, increasing bearing capacity, and reducing foundation settlement (Rajagopal and Murugesan, 2007; Murugesan and Rajagopal, 2009; Gniel and Bouazza, 2010; Ali et al., 2012; Ghazavi and Afshar, 2013; Miranda and Costa, 2016; Zhou et al., 2019; Ankit et al., 2020). These improved piles have proven effective in reinforcing soft soil foundations (Raithel et al., 2005; Lee et al., 2008; Gniel and Bouazza, 2009; Araujo et al., 2009; Indraratna et al., 2015; Chen et al., 2015; Alkhorshid et al., 2018; Ghanizadeh et al., 2023). However, the potential for using solid waste materials to construct granular piles, particularly concerning their bearing and deformation characteristics, has not been extensively explored.

This paper introduces and investigates a novel type of geotextile-encased granular pile composed of solid waste materials. Specifically, the pile consists of concrete granular material encapsulated in a geotextile ring, as illustrated in Figure 1. The study

involves physical experiments to assess the effects of concrete granular material and geotextile on the bearing and deformation characteristics of the piles. Additionally, model tests in soft clay are conducted to compare the bearing capacity performance of geotextile-encased granular piles with traditional granular piles.



(a) Geotextile-encased granular pile using recycled solid waste



(b) Concrete solid waste



(c) Ring geotextile

Figure 1. Composition of geotextile-encased granular pile using recycled solid waste

2 GEOTEXTILE-ENCASED GRANULAR PILE UNDER UNIAXIAL COMPRESSION

2.1 Sample Preparation

To assess the effects of concrete granular material and geotextile on the bearing and deformation characteristics of geotextile-encased piles, uniaxial compression tests were conducted. The sample piles comprised ring geotextile and concrete solid waste. The geotextile, made of polypropylene, was 1mm thick and had a diameter of 20cm. Four geotextiles with tensile strengths of 18kN/m, 52kN/m, 88kN/m, and 126kN/m were tested. Concrete waste, obtained from a construction waste treatment plant, was categorized into three particle sizes: 1–2cm, 2–3cm, and 3–4cm, as illustrated in Figure 2.

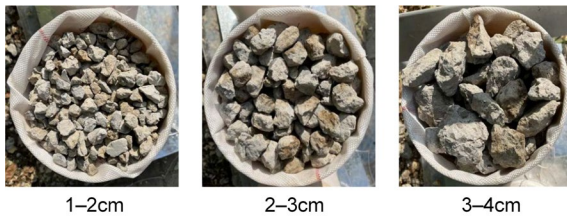


Figure 2. Particle sizes of concrete solid waste material

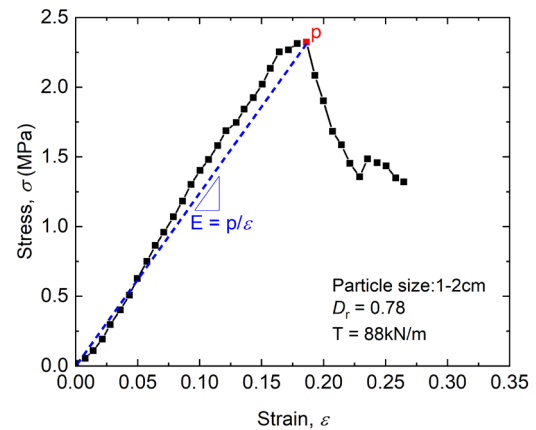
Specimens were prepared using a cylindrical acrylic mould, 40cm in height and 20cm in inner diameter. The geotextile was positioned inside the mould, fitting snugly against the walls. The granular material was then added and compacted by vibration to achieve uniform density. Once compacted, the mould and excess geotextile were carefully removed, leaving the finished pile specimen.

The specimens were tested using a universal testing machine, with a loading rate of 3.6mm/min for the uniaxial compression tests.

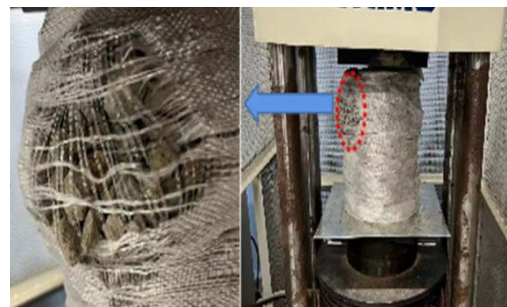
2.2 The stress-strain relationship of a typical test

A specimen was first made with particle size 1–2cm, soil relative density $D_r = 0.78$ and geotextile tensile strength $T = 88\text{kN/m}$. Then, a uniaxial compression test was carried out using the universal testing machine. The axial stress-strain relationship is shown in Figure 3(a). It can be seen that the stress increased nearly linearly with strain until reaching a peak, defined as the pile strength p . The pile strength p is $p = 2.32\text{MPa}$. As shown in this figure, the pile modulus $E = p/\epsilon$ can be assessed and equal to $E = 12.47\text{MPa}$.

Beyond this peak, the stress declined, indicating failure and strain softening. The failure mechanism, depicted in Figure 3(b), revealed that the granular material punctured the geotextile, leading to lateral deformation and structural degradation.



(a) Stress versus strain



(b) Failure mechanism of the specimen

Figure 3. Uniaxial compression test

2.3 Effect of Soil Relative Density (D_r)

The influence of soil relative density on pile performance was investigated by preparing specimens with a concrete particle size of 1–2cm and a geotextile tensile strength of 88kN/m. The relative densities were controlled at $D_r = 0.49, 0.62,$ and 0.78 . Figure 4 shows the axial stress-strain relationships for these densities. Both pile strength p and pile modulus E increased with increasing D_r . The pile strengths recorded were 2.18MPa, 2.21MPa, and 2.32MPa, with a corresponding modulus of 7.85MPa, 11.88MPa, and 12.47MPa, for D_r values of 0.49, 0.62, and 0.78, respectively. The relatively modest increase in pile strength with increasing D_r may be due to the similar geotextile puncture resistance and uniform particle size across the samples.

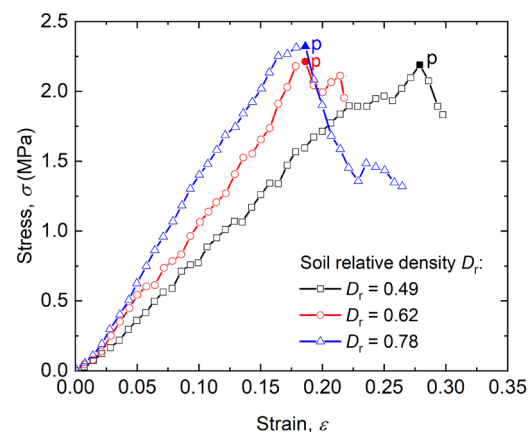


Figure 4. Stress versus strain considering various soil relative density

2.4 Effect of Particle Size

The effect of particle size was examined using three sizes: 1–2cm, 2–3cm, and 3–4cm. Figure 5 displays the stress-strain curves for these sizes. The piles with 1–2cm and 2–3cm particles exhibited similar strengths (2.40MPa and 2.34MPa, respectively) and modulus (12.0MPa and 12.3MPa, respectively). However, the pile with 3–4 cm particles showed a noticeable reduction in both strength (1.83MPa) and modulus (7.3MPa).

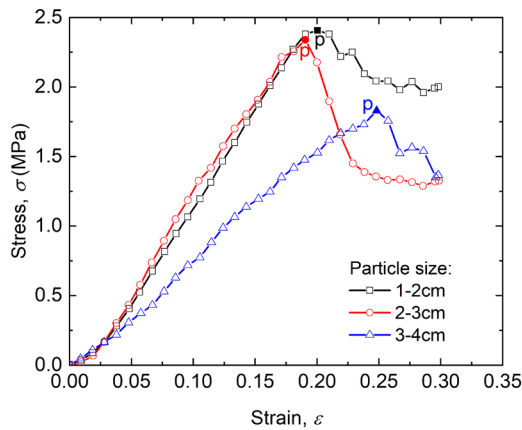


Figure 5. Stress versus strain considering various particle size

The larger particles were more prone to puncturing the geotextile, as seen in the failure mechanism (Figure 3(b)). This led to a lower pile strength and increased deformation. Additionally, the larger particles were more susceptible to crushing, as evidenced by the particle size distribution changes after testing (Figure 6). The increased proportion of smaller particles post-test indicated significant breakage of larger particles. Consequently, particles larger than 3cm are not recommended for use in geotextile-encased granular piles due to their tendency to cause greater geotextile damage and structural instability.

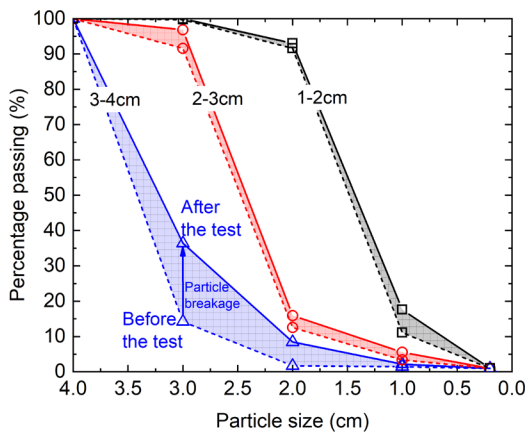


Figure 6. Particle breakage of granular pile specimens with different particle sizes

2.5 Effect of Geotextile Tensile Strength

The impact of geotextile tensile strength on pile behaviour was studied using geotextiles with tensile strengths of 18kN/m, 52kN/m, 88kN/m, and 126kN/m. The stress-strain curves are presented in Figure 7. As the tensile strength of the geotextile increased, the pile strength p also increased, highlighting the significant role of geotextile strength compared to soil relative density and particle size (1–3cm).

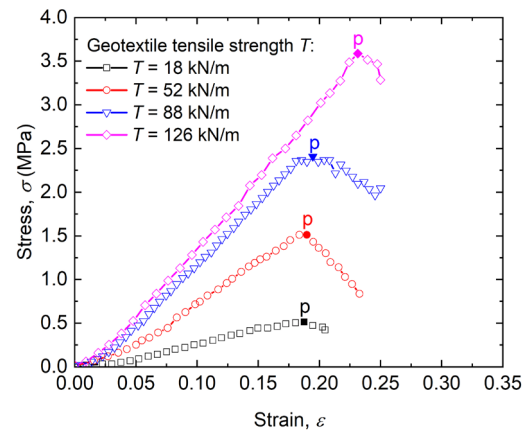


Figure 7. Stress versus strain considering various geotextile tensile strength

The relationships between pile strength p and pile modulus E with geotextile tensile strength are shown in Figure 8. These relationships can be modelled using the equations:

$$p = 0.028T \tag{1}$$

$$E = 26(1 - e^{-T/140}) \tag{2}$$

The equations show a good fit with the experimental data. For practical engineering applications, these equations can assist in selecting appropriate geotextile tensile strengths based on the desired bearing and deformation characteristics of the piles.

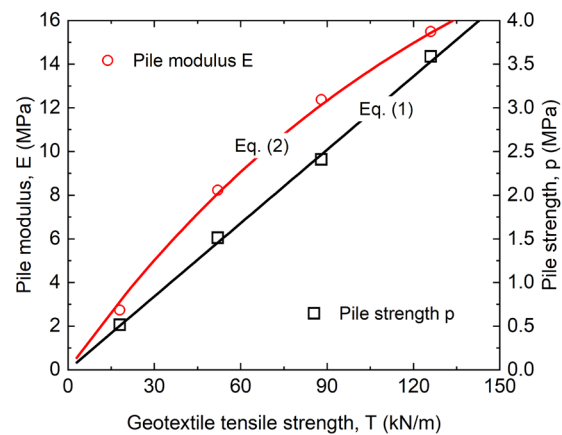


Figure 8. Pile modulus E and pile strength p versus geotextile tensile strengths T

3 THE PERFORMANCE OF GRANULAR PILE IN SOFT CLAY

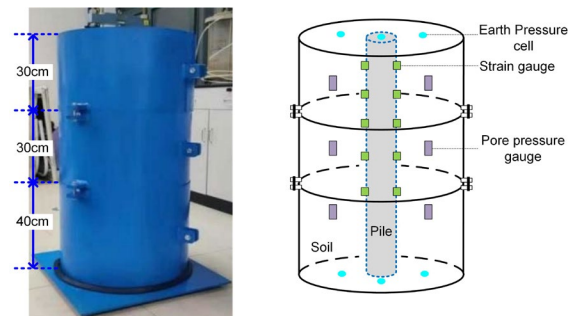
To evaluate the performance of geotextile-encased granular piles in soft clay, a series of model tests were conducted. This section describes the test design, procedures, and results.

3.1 Test Design and Procedure

The test piles, with a diameter of 0.1m and a length of 1m, utilized concrete solid waste material with a particle size of 1–2cm. Geotextiles with a tensile strength of 64kN/m were used for the encased piles. Kaolin clay, chosen for its fine particles and cohesive properties, was the soil medium. The properties of Kaolin soil include a plasticity index (Ip) of 23.7, a liquid limit (LL) of 46.5%, a consolidation coefficient (Cv) of 42.5m²/year, a permeability coefficient (k) of 3 × 10⁻⁸ m/s, and a void ratio (e) of 1.22.

The experimental setup comprised a model box, divided into three sections with heights of 30cm, 30cm, and 40cm, respectively (Figure 9(a)). Instrumentation included six earth pressure cells to measure stress distribution, ten strain gauges for monitoring deformation, and six pore pressure gauges to track pore water pressure during loading. This setup ensured comprehensive data collection on pile behaviour under load.

Static loading tests were conducted, as illustrated in Figure 9(b), following a six-step incremental loading protocol. Each step involved an incremental load of 6.4kPa, allowing for detailed observation of the load-settlement behaviour. Settlement measurements were taken using two displacement gauges.



(a) Model box and equipment layout diagram



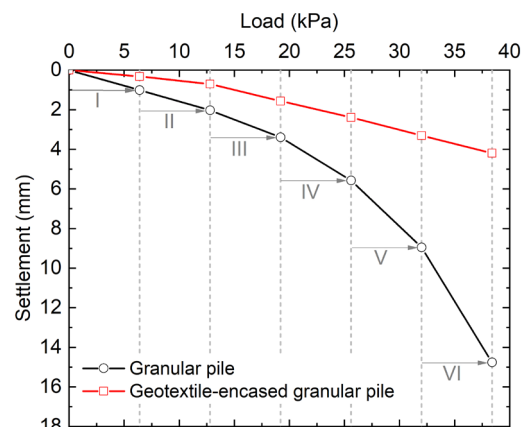
(b) Static loading test

Figure 9. Test procedure

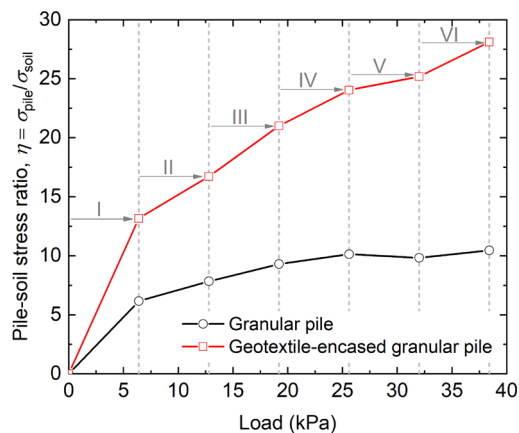
3.2 Test Results

The load-settlement behaviour of both granular piles and geotextile-encased granular piles was recorded and analysed. As shown in Figure 10(a), after applying a total load of 38.4kPa, the granular pile experienced a settlement of 14.8mm. In contrast, the geotextile-encased pile exhibited a significantly reduced settlement of 4.2mm, a 72% reduction. This outcome underscores the geotextile's role in enhancing the bearing capacity and reducing settlement.

Further analysis involved calculating the pile-soil stress ratios (η), defined as the ratio of the stress at the top of the pile (σ_{pile}) to the stress in the surrounding soil at the pile top (σ_{soil}), both measured by earth pressure cells. Figure 10(b) presents these ratios for both pile types as a function of the applied load. The stress ratio for the solid waste granular pile reached 28.1, while the geotextile-encased pile showed a much lower ratio of 10.4. This 176% increase in the pile-soil stress ratio for the geotextile-encased pile demonstrates the geotextile's effectiveness in distributing load and reducing stress on the surrounding soil.



(a) Load-settlement curves



(b) Pile-soil stress ratio

Figure 10. Comparison of bearing characteristics by model tests

The superior performance of the geotextile-encased granular pile can be attributed to several factors. The geotextile provides lateral confinement, preventing excessive lateral deformation and bulging, common failure modes in traditional granular piles. This confinement facilitates more efficient load transfer from the pile to the surrounding soil, improving overall stability and bearing capacity. Additionally, the geotextile helps distribute the applied load evenly along the pile's length, reducing stress concentrations and potential failure points.

Overall, the model tests indicate that geotextile-encased granular piles significantly outperform traditional granular piles in terms of settlement reduction and load distribution. These findings suggest that incorporating geotextiles into pile design enhances structural performance and durability, particularly in soft clay environments. The results provide a strong case for adopting geotextile-encased piles in practical engineering applications, offering a sustainable and efficient solution for foundation reinforcement.

4 CONCLUSION

This study investigates the bearing deformation performance of geotextile-encased granular piles using recycled solid waste through experimental tests, focusing on pile strength and modulus, and bearing capacity in soft clay.

Uniaxial compression tests revealed that higher geotextile tensile strength significantly increased pile strength and modulus, which had a larger sensitivity than soil relative density. Smaller particles (1–3cm) resulted in better performance, while larger particles (3–4cm) were prone to puncturing the geotextile and crushing, leading to decreased strength. These findings highlight the importance of incorporating geotextiles in pile design to enhance bearing capacity and reduce settlement. The use of 1–3cm concrete particles is recommended, and equations (1) and (2) can guide the selection of suitable geotextiles. Further research on long-term performance and the effects of different conditions is needed.

Model tests in soft clay showed that geotextile-encased granular piles had 72% lower settlement (4.2mm) compared to traditional granular piles (14.8mm) under the same loading. The geotextile-encased piles also exhibited a 176% higher pile-soil stress ratio, indicating improved load distribution and reduced stress on the surrounding soil.

In conclusion, geotextile-encased granular piles using recycled solid waste significantly improve pile strength and stability in soft clay, offering a sustainable solution for construction practices.

REFERENCES

- Ali, K., Shahu, J. T., and Sharma, K. G. (2012). "Model tests on geosynthetic-reinforced stone columns: a comparative study." *Geosynthetics International*, 19(4): 292-305.
- Alkhorshid, N. R., Araújo, G. L. S., and Palmeira, E. M. (2018). "Behavior of Geosynthetic-Encased Stone Columns in Soft Clay: Numerical and Analytical Evaluations." *Soils and Rocks*, 41(3): 333-343.
- Ankit, T., Saurabh, R., Ashok, K. G. (2020). "Experimental and numerical modelling of group of geosynthetic-encased stone columns." *Innovative Infrastructure Solutions*, 6: 1-17.
- Araujo, G. L. S., Palmeira, E. M., and Cunha, R. P. (2009). "Behaviour of geosynthetic-encased granular columns in porous collapsible soil." *Geosynthetics International*, 16(6): 433-451.
- Chen, J., Li, L., and Xue, J. (2015). "Failure mechanism of geosynthetic-encased stone columns in soft soils under embankment." *Geotextiles and Geomembranes*, 43(5): 424-431.
- Ghanizadeh, A. R., Ghanizadeh, A., Asteris, P. G., Fakharian, P., and Armaghani, D. J. (2023). "Developing bearing capacity model for geogrid-reinforced stone columns improved soft clay utilizing MARS-EBS hybrid method." *Transportation Geotechnics*, 38: 100906.
- Ghazavi, M., and Afshar, J.N. (2013). "Bearing capacity of geosynthetic encased stone columns." *Geotextiles and Geomembranes*, 38: 26-36.
- Gniel, J., and Bouazza, A. (2009). "Improvement of soft soils using geogrid encased stone columns." *Geotextiles and Geomembranes*, 27(3): 167-175.
- Gniel, J., and Bouazza, A. (2010). "Construction of geogrid encased stone columns: a new proposal based on laboratory testing." *Geotextiles and Geomembranes*, 28(1): 108-118.
- Indraratna, B., Ngo, N. T., Rujikiatkamjorn, C., and Sloan, S.W. (2015). "Coupled discrete element-finite difference method for analysing the load-deformation behaviour of a single stone column in soft soil." *Computers and Geotechnics*, 63: 267-78.
- Lee, D. Y., Yoo, C., Park, S., and Jung, S. (2008). "Field load tests of geogrid encased stone columns in soft ground." *Proceedings of the Eighteenth International Offshore and Polar Engineering Conference*, Vancouver, 521-524.
- Miranda, M., and Costa, A. D. (2016). "Laboratory analysis of encased stone columns." *Geotextiles and Geomembranes*, 44(3): 269-277.
- Murugesan, S., and Rajagopal, K. (2009). "Studies on the behavior of single and group of geosynthetic encased stone columns." *Journal of Geotechnical and Geoenvironmental Engineering*, 136(1): 129-139.
- Raithel, M., Küster, V., and Lindmark A. (2004). "Geotextile encased columns—a foundation system for earth structures, illustrated by a dyke project for a works extension in Hamburg." *Nordic Geotechnical Meeting*, Linköping, 1-10.
- Raithel, M., Kirchner, A., Schade, C., and Leusink, E. (2005). "Foundation of constructions on very soft soils with geotextile encased columns-state of the art." *Proceedings of GeoFrontiers*, Reston, 1-11.
- Rajagopal, K., and Murugesan, S. (2007). "Model tests on geosynthetic encased stone columns." *Geosynthetics International*, 14(6): 346-354.
- Zhou, Y., and Kong, G. (2019). "Deformation Analysis of Geosynthetic-Encased Stone Column-Supported Embankment considering Radial Bulging." *International Journal of Geomechanics*, 19(6): 04019057.